Front. Earth Sci. 2024, 18(2): 400–411
https://doi.org/10.1007/s11707-024-1101-6

RESEARCH ARTICLE

Machine learning methods for predicting the uniaxial compressive strength of the rocks: a comparative study

Tao WEN (✉)[1,2,3], Decheng LI[1], Yankun WANG[1,3], Mingyi HU[1,3], Ruixuan TANG[1,3]

1 School of Geosciences, Yangtze University, Wuhan 430100, China
2 Badong National Observation and Research Station of Geohazards, China University of Geosciences, Wuhan 430074, China
3 Jiacha County Branch of Hubei Yangtze University Technology Development Co., Ltd, Shannan 856499, China

Abstract The uniaxial compressive strength (UCS) of rocks is a critical index for evaluating the mechanical properties and construction of an engineering rock mass classification system. The most commonly used method for determining the UCS in laboratory settings is expensive and time-consuming. For this reason, UCS can be estimated using an indirect determination method based on several simple laboratory tests, including point-load strength, rock density, longitudinal wave velocity, Brazilian tensile strength, Schmidt hardness, and shore hardness. In this study, six data sets of indices for different rock types were utilized to predict the UCS using three nonlinear combination models, namely back propagation (BP), particle swarm optimization (PSO), and least squares support vector machine (LSSVM). Moreover, the best prediction model was examined and selected based on four performance prediction indices. The results reveal that the PSO–LSSVM model was more successful than the other two models due to its higher performance capacity. The ratios of the predicted UCS to the measured UCS for the six data sets were 0.954, 0.982, 0.9911, 0.9956, 0.9995, and 0.993, respectively. The results were more reasonable when the predicted ratio was close to a value of approximately 1.

Keywords uniaxial compressive strength, particle swarm optimization, least squares support vector machine, prediction model, prediction performance

1 Introduction

The UCS of intact rocks is a vital parameter for rock mass quality evaluation and stability of underground excavations (Aladejare, 2020; Iyare et al., 2021; Wen et al., 2021, 2023). The direct method for measuring UCS in laboratory tests is relatively expensive and troublesome (Mohamad et al., 2018; Hu et al., 2021; Zhang et al., 2022). Thus, adopting an effective and reliable method to estimate the UCS is very important (Abdi et al., 2020). At present, an indirect method for determining UCS is often of interest and popularity. For example, an estimation of UCS based on simple rock indices is conducted by some prediction models, including simple and multiple-regression analysis techniques, etc. (Jahed Armaghani et al., 2016; Rahman and Sarkar, 2021).

Considerable attempts to estimate the UCS of rocks based on their intended use have had certain progress (Momeni et al., 2015a; Rahman and Sarkar, 2021; Zhang et al., 2022). UCS is grounded on physical and mechanical properties including density, point-load strength, tensile strength, longitudinal wave velocity, etc (Zhang et al., 2022). To determine UCS more accurately, many effective and rapid methods for determining the UCS of rocks have been adopted by statistical regression models or intelligent optimization algorithms (Jahed Armaghani et al., 2016; Mohamad et al., 2018). With their efficiency in nonlinear modeling, machine learning (ML) algorithms can capture complex behavior-influencing parameters, providing viable tools for simulating many complex problems. In the past, various ML algorithms, such as artificial neural networks (ANN), adaptive neuro-fuzzy inference system (ANFIS), extreme gradient boosting machine (XGBoost), extreme learning machine (ELM), support vector machine (SVM), etc., have been used to estimate the desired output. Table 1 presents the existing methods used to predict UCS. They employ various artificial intelligence algorithms and selected physical and mechanical parameters, such as porosity, density, and wave velocity, as input parameters. Furthermore, the Schmidt hammer rebound number is one of most important parameters in estimating other parameters

Received February 4, 2023; accepted July 21, 2023

E-mail: wentao200840@yangtzeu.edu.cn

Table 1 Some of existing studies in field of rock strength prediction

References	Prediction models	Input parameters	Output parameters	Samples
Mohamad et al. (2015)	PSO-ANN	BTS, Is(50), Vp, DD	UCS	40
Momeni et al. (2015b)	PSO-ANN	Rn, Vp, Is(50), DD	UCS	66
Jahed Armaghani et al. (2016)	ICA-ANN	Rn, Vp, Is(50)	UCS	108
Jahed Armaghani et al. (2016)	NLMR, ANN, ANFIS	Rn, Vp, Is(50)	UCS	124
Li and Tan (2016)	MLR, LSSVM	TS, Vp, Is(50),DD	UCS	24
Mohamad et al. (2018)	PSO-BP	Vp, Is(50), DD, MC,Id2	UCS	38
Abdi et al. (2020)	PSO-ANN	Rn, Vp, DD	UCS	60
Aladejare (2020)	Several empirical equations	Is(50), n_e, DD, BPI, SHH	UCS	60
Li et al. (2020)	GMDH	Rn, Vp, DD	UCS	86
Teymen and Mengüç (2020)	SRA, MRA, ANN, ANFIS, GEP	BTS, Vp, Is(50),DD, SHH, SSH	UCS	93
Gowida et al. (2021)	ANN, ANFIS, SVM	ROP, GPM, SPP, RPM, T, WOB	UCS	1771
Zhang et al. (2022)	GA-SEL	Vp, Is(50), BPI, Rn	UCS	166
Liu et al. (2022)	XGBoost	Rn, Vp, Is(50)	UCS	108
Skentou et al. (2023)	ANN-LM, ANN-PSO, ANN-ICA	Rn, Vp, n_e	UCS	274

Notes: Point load indice test (Is(50)), Schmidt hammer rebound number (Rn), p-wave velocity test (Vp) and dry density (DD), Effective porosity (n_e), Brazilian Tensile strength (BTS), moisture content (MC), slake durability indice (Id2) (second cycle), Schmidt hardness (SHH), Shore hardness (SSH), block punch indice (BPI), rate of penetration (ROP), mud pumping rate (GPM), standpipe pressure (SPP), rotary speed in revolution per minute (RPM), torque (T), and weight on bit (WOB).

(Asteris et al., 2021). For the ANN model, implementing more than one hidden layer increases the likelihood of model overfitting and overtraining when the size of the data set is small (Jahed Armaghani et al., 2016). The ANFIS network node functions have almost no constraints other than piecewise differentiability from a functional perspective. However, from a structural perspective, the only limitation on network configuration is that it should be a feedforward network (Gowida et al., 2021). An indirect method for determining the UCS is very helpful in the initial design stage of rock engineering (Teymen and Mengüç, 2020). However, the use of empirical formulas may result in underestimating or overestimating the UCS of a particular site (Rahman and Sarkar, 2021). Since empirical formulas are proposed for different rock types of different rock geneses or based on smaller regions, most empirical equations have special characteristics. In addition, the expression of the strength transformation equation is dispersive, limiting the application of empirical models (Aladejare, 2020; Zhang et al., 2022). With the development of artificial intelligence, many machine learning methods can help solve multivariable and nonlinear complex problems (Gowida et al., 2021; Wang et al., 2022). They are utilized to predict UCS when integrated with other optimization methods, and have effectively been employed in rock engineering. Nevertheless, different models have certain adaptability to different data sets. It is a difficult process to find a suitable and effective model and its super parameters, which usually depends on a rich machine learning algorithm experience.

As shown previously, many prediction methods have been employed for specific cases applicable to estimating the UCS of different rock types. Nevertheless, the predicted results of these methods are more or less imperfect, and little information on different rock types or rocks from different places has been presented in previous research. Based on the above-mentioned research, a reasonable and applicable UCS determination method should process certain physical aspects to reflect the relationship between the rock physical or mechanical properties and the UCS. Herein, three nonlinear combination methods were employed for determining UCS using several rock indices. The predicted results were compared with the measured results. Additionally, the best prediction method was employed to be utilized for engineering practices.

2 Methodology

2.1 Back propagation (BP)

Neural networks are usually used as an alternative method to supersede autocorrelation, linear regression, multivariable regression, etc (Zhang et al., 2024). In the category of information, a multifunctional neural network is regarded as an expert source that can be used to offer projections, given new solutions. The BP algorithm is one of the most commonly used neural network algorithms, which is popular in various engineering fields (Li et al., 2014). The principle of BP lies in employing the gradient descent method to progressively modify the weight and threshold of the network via back propagation, and the purpose is to minimize the sum of network error squares.

The topological structure of the BP algorithm contains a large number of nodes called neurons and the interconnection between input (IL), hidden (HL), and output layers (OL). A node in the IL symbolizes a key parameter, while the node in the OL symbolizes the generated predicted value following network analysis. The HL is used to insert several layers of neurons between the IL and the OL to increase the interconnection between the IL and the OL, thus complicating the network and enhancing the prediction ability of the BP model. The neurons between each layer are fully connected through the link, which can be stored as a weighted standard value to measure the connection between each node. The weight can be changed to minimize the error function, and the weight can be updated in reverse during the process of minimizing the error function.

2.2 Least squares support vector machine (LSSVM) algorithm

The principle of the support vector machine (SVM) is switching the input space into a high-dimensional space employing nonlinear transformation and searching the optimal linear classification hyperplane in the new space. The SVM algorithm has global optimality and strong generalization ability, which can solve the problem of small-sample learning. The LSSVM is a modified SVM algorithm, which is utilized to mine data, distinguish patterns, etc (Cai et al., 2016; Wen et al., 2017; Zhu et al., 2018). In the LSSVM algorithm, the loss of function is determined based on the linear least squares criterion, and the sum of error squares is considered the loss of function of the training samples. By transforming the inequality constraints of the SVM algorithm into equality constraints, a system of linear equations is obtained to solve the quadratic optimization problem. According to the literature (Cai et al., 2016; Wen et al., 2017; Zhu et al., 2018), both the kernel parameter σ^2 and regularization parameter γ have significant influences on the validation performances of the LSSVM algorithm. The parameter γ determines the training error, while σ^2 influences a nonlinear mapping relationship from the input space to a high-dimensional space. The training error gradually decreases with an increasing γ. If this value is large enough, the model will be complex and time-consuming. The σ^2 value represents the shape of a bell-type function in the high-dimensional space. However, there is still no normative method to determine the parameters at present, and the usual way is to obtain better prediction performance through exploratory debugging parameters. Therefore, the parameters should be optimized to enhance the prediction precision via other intelligent optimization algorithms.

2.3 Particle swarm optimization (PSO) algorithm

The PSO algorithm is an important branch of an intelligent algorithm, overcoming optimization problems of evolutionary population (Mohamad et al., 2015). PSO is also regarded as a direct and capable global optimization algorithm (Mohamad et al., 2018). In PSO, each particle symbolizes a possible solution based on the speed–position search model (Abdi et al., 2020). The quality of each particle is assessed by the fitness function. Suppose that in a population composed of n particles in the d-dimensional space, each particle approaches two points. The first point is regarded as the optimal solution achieved by all particles in the entire particle swarm in the search process of previous generations, which is called the global optimal solution, g_{best}. The other point is also considered the optimal solution that each particle has reached in the search process of previous generations, which is described as an individual optimal solution, p_{best}. Suppose that the ith particle has a certain position $x_i = (x_{i1}, x_{i2}, L, x_{id})$ and a certain flight speed $v_i = (v_{i1}, v_{i2}, L, v_{id})$, the optimal position of the ith particle is $p_{\text{best}} = (p_{i1}, p_{i2}, L, p_{id})$ and the global optimal position of all particles is $g_{\text{best}} = (g_1, g_2, L, g_d)$ based on the criterion that its advantages and disadvantages are evaluated by the fitness value of each particle. Afterward, each particle is evaluated by modifying the velocity and position of the particles in the next iteration according to Eqs. (1) and (2).

$$v_{id}^{k+1} = w_k v_{id}^k + c_1 rand_1(p_{id}^k - x_{id}^k) + c_2 rand_2(g_d^k - x_{id}^k), \quad (1)$$

$$x_{id}^{k+1} = v_{id}^{k+1} + x_{id}^k, \quad (2)$$

where k is the kth iteration; $i = 1, 2, L, n$; c_1 and c_2 are acceleration constants, usually 2; $rand_1$ and $rand_2$ are independent random numbers, ranging from 0 to 1; v_{id}^k is the d-dimension component of the velocity vector of particle i in the kth iteration; x_{id}^k is the d-dimension component of the position vector of particle i in the kth iteration; p_{id}^k is the d-dimension component of the optimal position of particle i in the kth iteration; g_d^k is the d-dimension component of the optimal positions of all particles in the kth iteration; w_k is the inertia weight of the kth iteration.

2.4 PSO–BP

Due to the disadvantages of BP, PSO is used to improve the prediction precision of the BP algorithm by initializing some randomly selected particles. The combination algorithm can be simply described as follows.

1) First, in the BP algorithm, the parameters should be initialized.

2) Then, the initial weights and thresholds should be extracted. These parameters are encoded into a group of particles in the PSO algorithm, and the position and

random velocity of each particle are obtained.

3) The fitness of the particles by using training data should be calculated based on Eq. (3):

$$F = k\left(\sum_{i=1}^{n} asb(y_i - o_i)\right). \quad (3)$$

4) If the fitness value is better than the p_{best}, the value is used to replace the p_{best}. Similarly, if its fitness value is better than the g_{best}, the value is used to replace the g_{best}.

5) Then, in each particle, the position and random velocity should be modified by Eqs. (1) and (2).

6) An automatic calculation will stop when the error is within the allowable range.

Finally, in the BP algorithm, the initial weights and thresholds are replaced with the optimal weights and thresholds obtained by the PSO algorithm.

Furthermore, the training frequency, the learning rate and the population size should be set for all rock type data sets. The flow chart of the PSO-BP model is presented in Fig. 1.

2.5 PSO-LSSVM

To establish a reliable strength prediction model based on the LSSVM algorithm, some measures should be taken to pre-process training data and optimize the parameters. Herein, the PSO is utilized to adjust the regularization parameter γ and kernel parameter σ^2 in the LSSVM algorithm. The combination algorithm can be simply described as follows (Zhao et al., 2014; Xue and Xiao, 2017).

1) A set of the training samples in the LSSVM algorithm should be determined and the pre-process data should be handled;

2) The range of the regularization parameter γ and kernel parameter σ^2 should be determined and the particle dimension of the particle swarm should be set. Afterward, the velocity and position of particles will be generated randomly;

3) Then, each particle is set as the parameter of the LSSVM algorithm, and the prediction model is constantly being trained, so the predicted result can be output;

4) The output results are substituted into fitness evaluation functions to achieve the maximum number of iterations or acquire the global optimal solution. If the predicted result meets the maximum iterations or the global optimal solution, step 5 is omitted, otherwise step 5 should be performed;

5) Based on the fitness value of each particle, the position of the particle should be updated by the iterative equations;

6) The acquired optimal solution should be introduced into the LSSVM algorithm, and finally, an accurate

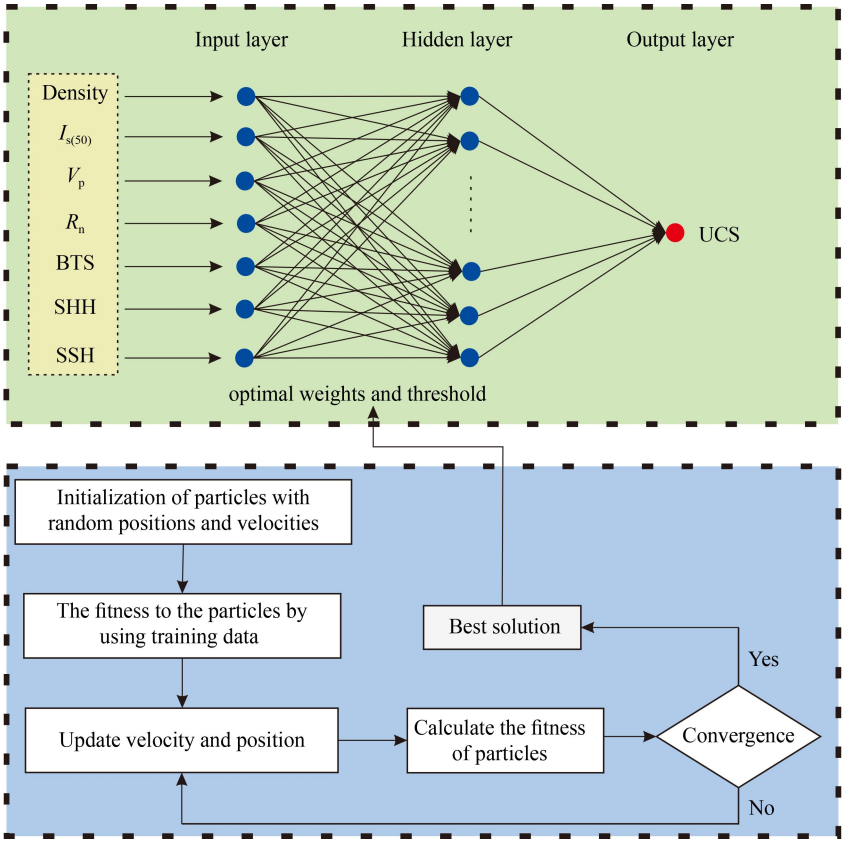

Fig. 1 The flow chart of the PSO-BP model.

prediction model should be built.

Furthermore, the training frequency, the learning rate and the population size should also be set for all rock type data sets. The flow chart of the PSO-LSSVM model is presented in Fig. 2.

2.6 Prediction performance measure

In this study, the BP, PSO–BP, and PSO–LSSVM models are employed for three different models to predict the UCS. To ensure that each model processes properly, some formulas must be adopted to assess the applicability of these models. Herein, four indices, including the coefficient of determination (R^2), root mean square error (RMSE), variance accounted for (VAF), and mean absolute error (MAE), were utilized to compare the predicted results obtained by different models.

$$R^2 = 1 - \frac{\sum_{i=1}^{N}(y - y')^2}{\sum_{i=1}^{N}(y - \bar{y})^2}, \tag{4}$$

$$\mathrm{RMSE} = \sqrt{\sum_{i=1}^{N}(y - y')^2}, \tag{5}$$

$$\mathrm{VAF} = \left[1 - \frac{\mathrm{var}(y - y')}{\mathrm{var}(y)}\right] \times 100, \tag{6}$$

$$\mathrm{MAE} = \frac{1}{N}\sum_{i=1}^{N}|y - y'|, \tag{7}$$

where y, y', and $\bar{y}$ are the tested value, the predicted value, and the mean value of parameter y, respectively; N is the total number of test data; var(y) is the variance of parameter y. Therefore, a model with an R^2 of 1, RMSE of 0, or VAF of 100, was regarded as a suitable model for predicting the UCS within the current data set. For the MAE, the significance of the model increases when the MAE decreases. In particular, the model can be considered strong and acceptable when the MAE is less than 10.

2.7 Differences between the three models

The feasibility of the three models can be validated based on the four indices mentioned above. The reliability of the prediction results of a model is closely related to its advantages and disadvantages. Therefore, the key differences of the three models are summarized in Fig. 3. According to the advantages and disadvantages of the BP and LSSVM algorithms, any method directly predicting landslide displacement will not obtain satisfactory results. Aiming at the disadvantages of the BP algorithm, the PSO algorithm is used to optimize the initial parameters of the BP algorithm. The PSO algorithm has the advantages of fewer parameters, fast convergence speed, and strong global search ability. The advantage is that the global search ability of the PSO algorithm is well-utilized to overcome the shortcomings of the LSSVM algorithm in parameter selection. By comparing the advantages and disadvantages of the models, the prediction accuracy of the combining model is better. In addition, the prediction accuracy of the PSO–LSSVM model was expected to be the best, while the prediction accuracy of the BP model the worst.

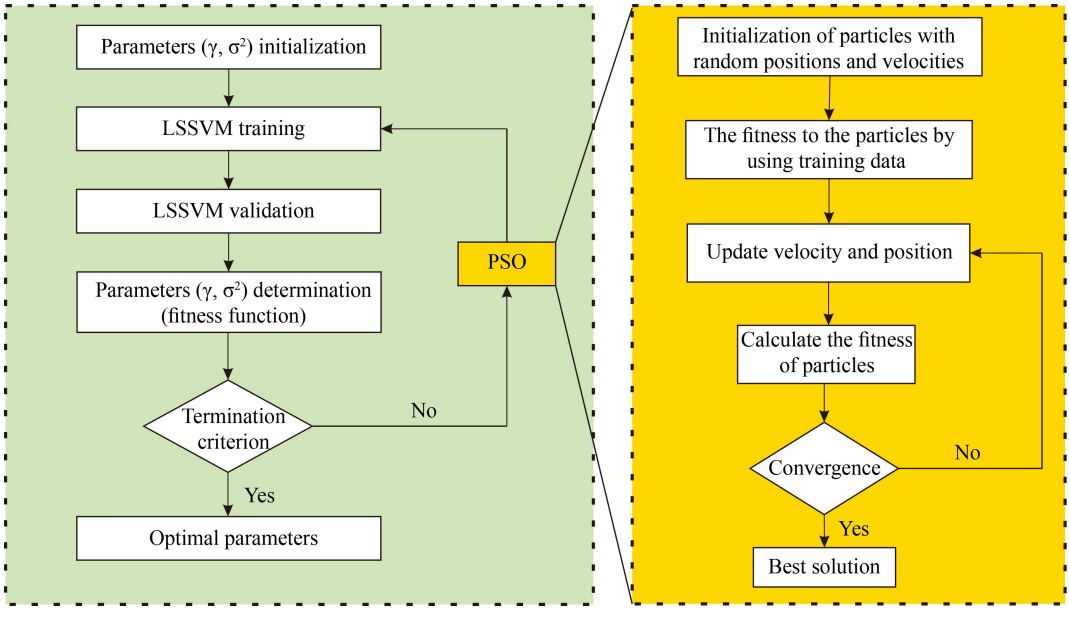

Fig. 2 The flow chart of the PSO-LSSVM model.

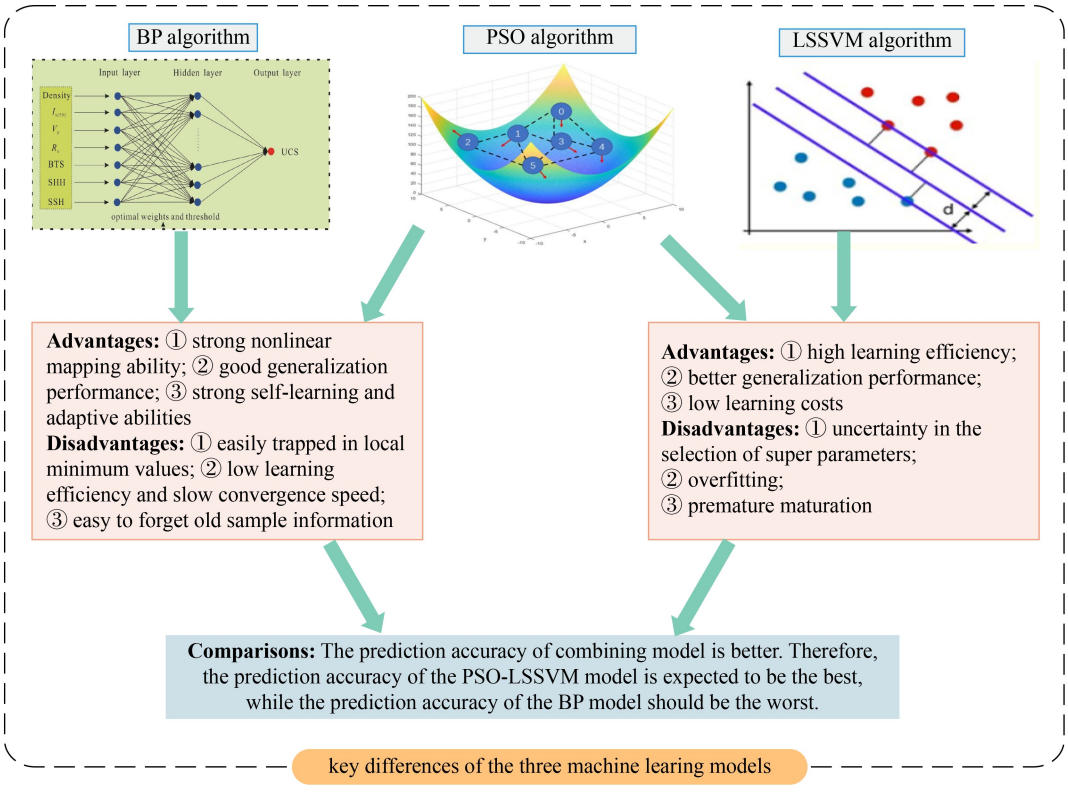

Fig. 3 Key differences of the three models.

3 Data set description

The rocks used in the study were collected from different literature, and a total of six data sets for different rock types were utilized to predict their uniaxial compressive strengths via different models. The tested rocks included shale, sandstone, volcanic rock, and granite. The preparation and testing process of these rocks complied with standard laboratory test procedures proposed by the ISRM. Information including rock density, point-load strength ($I_{s(50)}$), longitudinal wave velocity (V_p), and UCS, is provided for 24 data sets of shale samples (Li and Tan, 2016) and 38 data sets of sandstone samples (Mohamad et al., 2018). Data sources, rock density, $I_{s(50)}$, V_p, and UCS are provided for 20 data sets of volcanic rock samples (Teymen and Mengüç, 2020). The $I_{s(50)}$, V_p, UCS, and Schmidt hammer rebound number (R_n) are provided for 52 data sets of slightly weathered granite samples (Jahed Armaghani et al., 2016). Information including the UCS, rock density, shore hardness (SSH), Schmidt hardness (SHH), Brazilian tensile strength (BTS), $I_{s(50)}$, and V_p is provided for 87 data sets of volcanic rock samples (Teymen and Mengüç, 2020). Furthermore, the $I_{s(50)}$, V_p, UCS, and R_n are provided for 124 data sets of granite samples with different degrees of weathering (Jahed Armaghani et al., 2016). Herein, the rock density, $I_{s(50)}$, V_p, R_n, BTS, SHH, and SSH were considered as the input variables, and the UCS was utilized as the output variable in these models.

4 Results

Figure 4 shows the relationship between the UCS and different parameters. Herein, 87 data sets were taken as examples to represent these relationships. The results indicate that their relationships are statistically meaningful and acceptable. These parameters have a strong correlation with the rock strength. In particular, both $I_{s(50)}$ and BTS have good linear relationships with the UCS. Therefore, these parameters are sufficient for predicting the UCS. In conclusion, multi-input variables should be selected to estimate the UCS.

To determine the UCS of different rock types using the BP, PSO–BP, and PSO–LSSVM methods, the data sets were divided into training data and validation data. The training data were utilized to optimize the network, but the validation data were employed to evaluate the prediction precision of the models. Usually, 70% to 80% of the data sets should be used for training and 20% to 30% of the data sets should be used for testing (Looney, 1996; Jahed Armaghani et al., 2016). Complying with these suggestions, 75% to 80% of the data sets were used for training the model in this study, whereas 20% to 25% of the data sets were used for testing. In this study, 18 data sets were used for training the three models, while the remaining 6 data sets were used for testing these models. Thirty data sets were used for training the three models, while the remaining eight data sets were used for testing these models. Sixteen data sets were used for

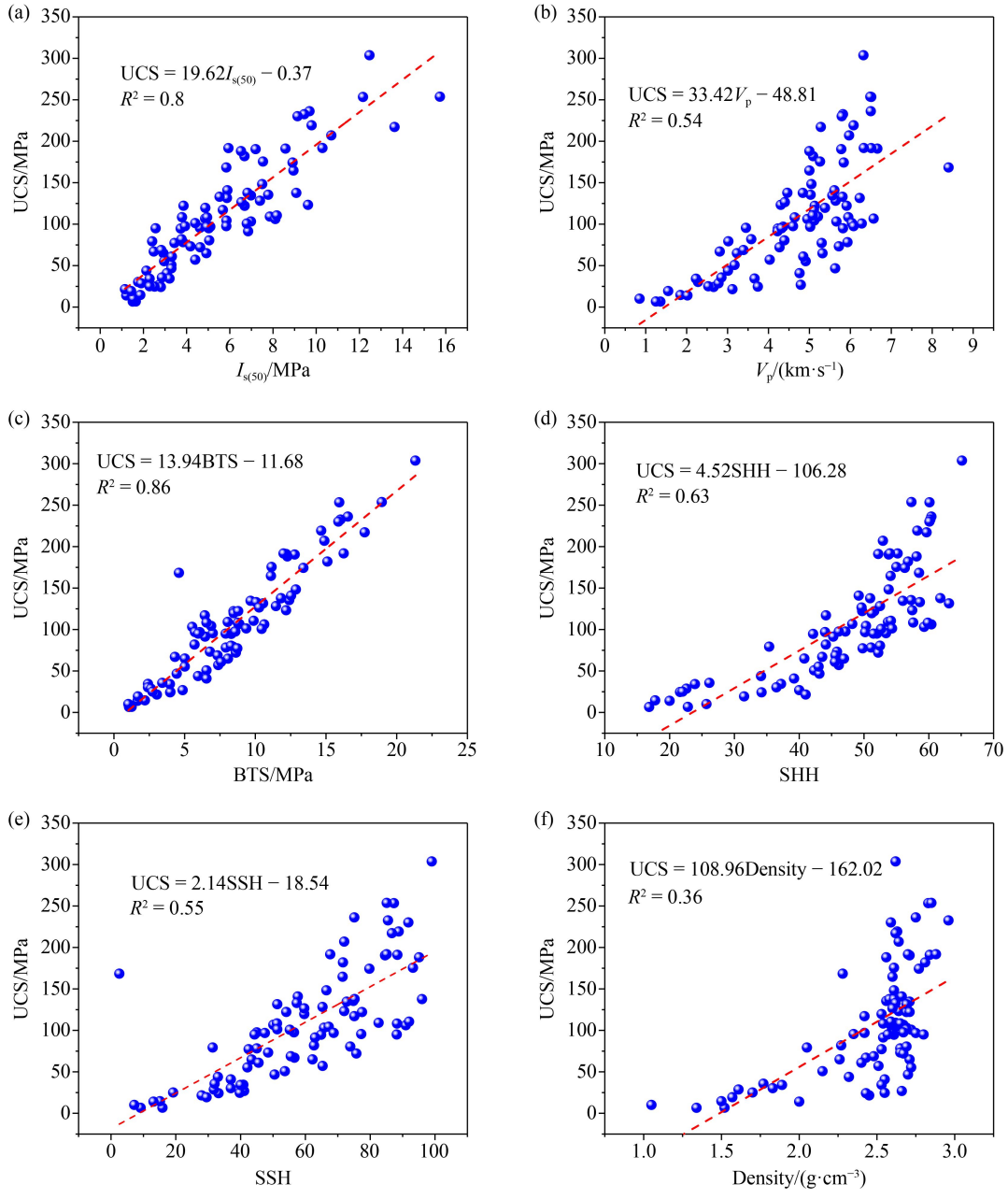

Fig. 4 Relationships between different parameters and the measured UCS for different rock types from different places: (a) $Is_{(50)}$; (b) V_p; (c) BTS; (d) SHH; (e) SSH; (f) density.

training the three models, while the remaining four data sets were used for testing these models. Furthermore, 41 data sets were used for training the three models, while the remaining 11 data sets were used for testing the models. For different rock types from different places, 70 data sets were used for training the three models, while the remaining 17 data sets were used for testing these models. For granite with different degrees of weathering, 99 data sets were used for training the three models, while the remaining 25 data sets were used for testing these models.

In the BP model, the training frequency was 2000 and the learning rate 0.0125 for all rock type data sets. Furthermore, the training frequency in the PSO–BP model was also set as 2000, the learning rate 0.0125, and the population size as 20 for all rock type data sets. These parameters of the PSO–LSSVM model were the same as that of the PSO–BP model.

Figure 5 exhibits the predicted results of the UCS. Compared with the measured values, the predicted values for the three models present similar trends with them, whereas the results determined by the PSO–LSSVM model exhibit better uniformity with the measured values than the other two models. Moreover, the predicted

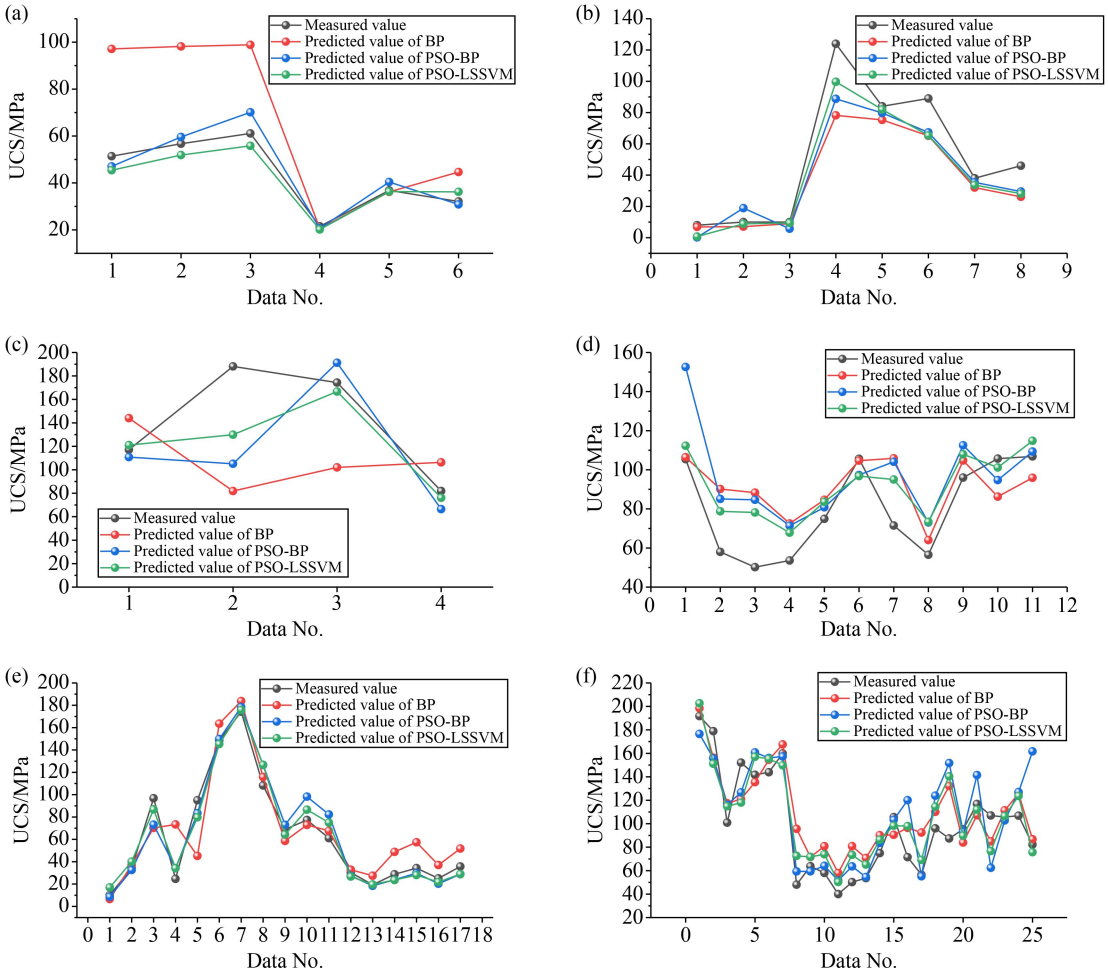

Fig. 5 Measured value and predicted value of the UCS for testing data at different rock types: (a) shale; (b) sandstone; (c) volcanic rock; (d) slightly weathered granite; (e) different rock types from different places; (f) granite with different weathered degrees.

results obtained by the PSO–BP model were better than those by the BP model. The advantages of the PSO–LSSVM model were especially clear from shale and sandstone, as shown in Figs. 5(a), 5(b), and 5(e), with the UCS exhibiting good agreement with the major influencing factors, including the $I_{s(50)}$, V_p, and BTS parameters. These curves of the predicted values were very well matched with the curves of the measured values. Though Fig. 5(c) does not show a good match, its difference was less than the other two models. Notably, for data No. 2 in Fig. 5(c), the predicted results were different from the measured results among the three models, but the predicted results determined by the PSO–LSSVM model were still the closest to the measured values. In Figs. 5(e) and 5(f), the predicted curves of the three models were close to the measured curves, and their error values were relatively small. However, the predicted results determined by the PSO–LSSVM model were still the closest to the measured values. The reason why the predicted values of the three models were all relatively small was that the amount of training data increases and is more suitable to find the optimal predicted parameters for debugging these models. Therefore, the optimal solution of the model was not only related to the influencing factors, but also to the amount of data.

The rationality of different models for the UCS prediction was evaluated by the R^2, RMSE, VAF, and MAE, as presented in Table 2. For the error analysis of the predicted results of slightly weathered granite and different rock types from different places, the four performance indices obtained by the PSO–LSSVM model were superior to those in the other two models. For the data of sandstone and volcanic rock, in the PSO–LSSVM model, the RMSE, VAF, and MAE values performed better than the other two models. In contrast, the performance indice R^2 was not optimal. For the data of granite with different degrees of weathering, in the PSO–LSSVM model, the R^2, RMSE, and MAE values produced better results than the other two models. On the other hand, the performance indice VAF was not optimal. In terms of the predicted results, the most unfavorable data set was that of shale for the PSO–LSSVM model. As just the R^2 value of the PSO–LSSVM model was larger

Table 2 The error analysis of the predicted results for the three models

Types	R^2			RMSE			VAF			MAE		
	BP	PSO-BP	PSO-LSSVM	BP	PSO-BP	PSO-LSSVM	BP	PSO-BP	PSO-LSSVM	BP	PSO-BP	PSO-LSSVM
1	0.92	0.95	0.96	21.33	7.88	8.70	93.85	93.09	85.74	7.33	0.54	2.67
2	0.94	0.97	0.96	42.00	17.82	5.82	77.52	93.04	95.26	6.21	0.80	0.71
3	0.76	0.82	0.67	80.07	63.51	4.64	36.10	73.23	95.22	16.45	11.85	0.47
4	0.39	0.49	0.83	48.40	40.55	3.46	74.78	67.00	95.66	3.70	3.62	0.16
5	0.81	0.95	0.97	86.82	46.70	35.95	97.85	94.47	98.57	4.54	0.96	0.45
6	0.77	0.64	0.79	110.06	139.12	99.63	30.80	38.00	33.82	9.28	9.59	6.37

than that of the other two models, other performance indices, including the RMSE, MAE, and VAF, were not optimal. On the whole, the PSO–LSSVM model was suitable for UCS prediction, and assisted in the evaluation of rock mechanics and classification of rock mass engineering.

To investigate the superiority of evaluation results from different models, the ratios of the predicted UCS to the measured UCS for six data sets are displayed in Fig. 6. The black line in this figure denotes the contour line between the measured UCS and the predicted UCS, while the yellow region denotes that the predicted UCS is within the upper/lower limit of 90%. The linear least squares method was used to fit all data sets from different rock types. In the PSO–LSSVM model, the predicted values were closely distributed around the contour line and were all within the range of the upper/lower limit of 90%. Following that, most predicted values in the PSO–BP model were within the range of the upper/lower limit of 90%. However, in the BP model, the predicted values were scattered on both sides of the contour line and a considerable part of them were outside the range of the upper/lower limit of 90%. Most prediction points were between the upper and lower limits of 80%. The results illustrate that the ratios of the predicted UCS to the measured UCS for six data sets were 0.954, 0.982, 0.9911, 0.9956, 0.9995, and 0.993, respectively. Fig. 6 shows that the predicted values of the PSO–LSSVM model are similar to the measured values. Compared with the other two models, the ratios of the predicted UCS to the measured UCS for six data sets with a value of approximately 1 were more reasonable. Although the performance of a linear fit of all data sets for the PSO–BP model was not as good as that for the PSO–LSSVM model, the fitted results still had some significance in predicting the UCS. Moreover, Figs. 6(e) and 6(f) exhibit that the PSO–LSSVM model also worked well for different rock types from different places, and granite with different degrees of weathering. Therefore, the PSO–LSSVM model was suitable for determining the UCS of different rock types.

In conclusion, the predicted results determined using BP and LSSVM after PSO were close to the measured results, which generally reflect the distribution of the UCS of rocks. However, these algorithms had their shortcomings. First, the BP model used the gradient descent method, so that the learning results heavily depended on initial weights. However, the selection of the initial weights of the BP model appeared to be unfounded, which led to network oscillation or non-convergence once the value was improper. Even if the value was converged, the training time would increase, seriously affecting the network generalization ability. Afterward, the sum of squares of the least squares linear system errors was assigned as the loss of function in the LSSVM model, which turned the solving process into solving a set of equations. This led to faster solution speed and fewer computing resources required for the solution; therefore, it achieved good results in the application of pattern recognition and nonlinear function fitting. However, the prediction precision of the LSSVM model was decided by the selection of its parameters, and its value was mainly based on experience and trial calculation, without unified rules. The PSO algorithm that was easy to implement and simple in concept was a parallel global search strategy based on population. In the PSO model, there were not many parameters to be adjusted. The algorithm possessed fast convergence speed and had certain advantages in dealing with high-dimensional problems. It was widely used in support vector machine parameter optimization. Therefore, PSO was utilized to optimize the BP and the LSSVM parameters in the study, and combining the phase space reconstruction theory to preprocess the data, both PSO–BP model and PSO–LSSVM models were established to predict the UCS of different rocks. The rationality and applicability of the two combination models were verified by a variety of test data for different rock types, and the PSO–LSSVM model was the most suitable for predicting rock strength.

5 Discussions

The UCS of a rock is a crucial parameter in geotechnical engineering, rock mechanics, and geology (Wen et al. 2023). It describes the ability of a rock to resist compressive stress, which can be important in a variety of

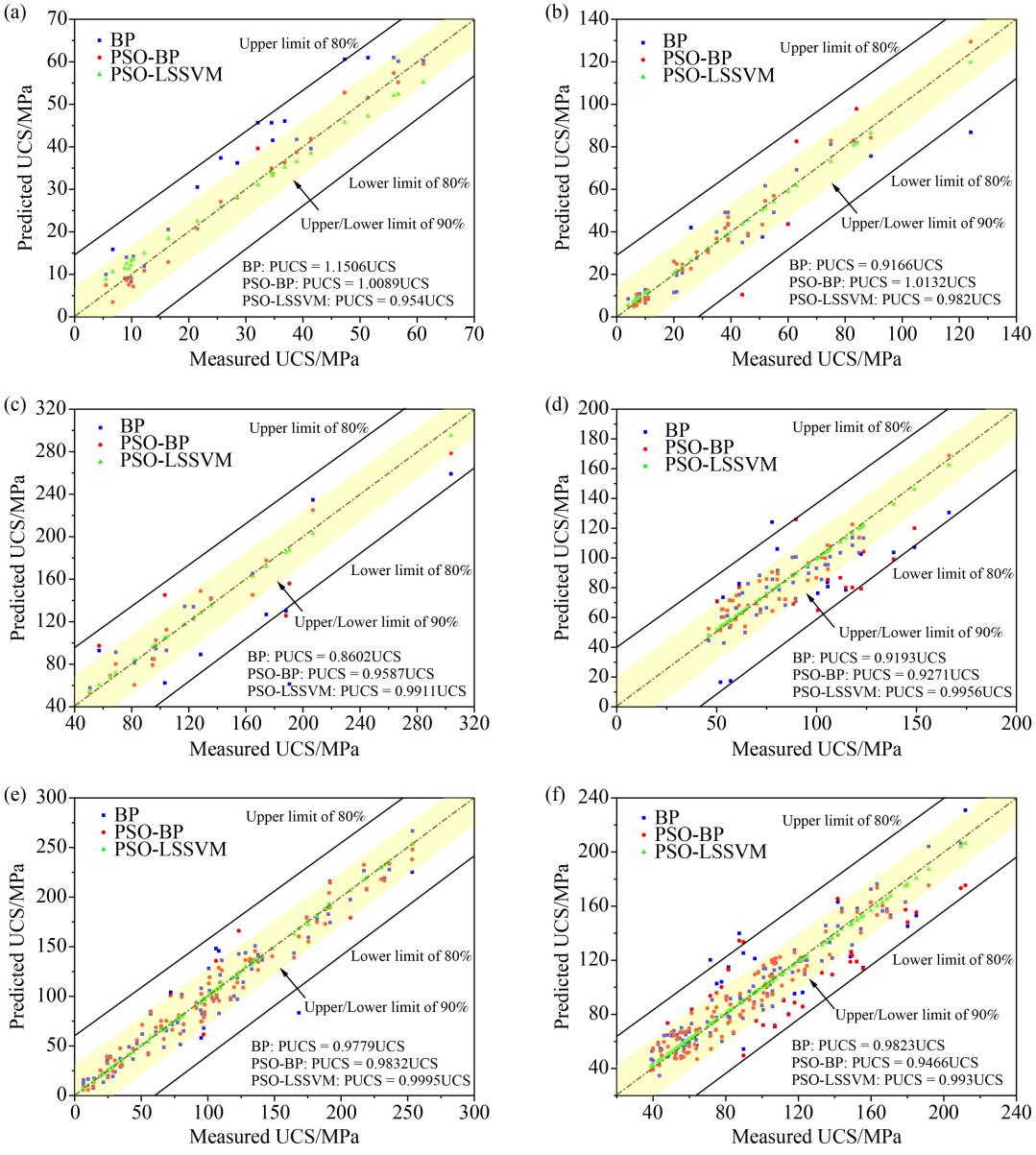

Fig. 6 Measured UCS and predicted UCS for training data and validation data at different rock types: (a) shale; (b) sandstone; (c) volcanic rock; (d) slightly weathered granite; (e) different rock types from different places; (f) granite with different weathered degrees.

applications, including stability assessments of rock masses, design of drilling and excavation tools, prediction of mining subsidence, and assessment of reservoir rock quality. Overall, predicting the UCS of geological formations is critical for designing reliable and safe geotechnical structures, efficient drilling and excavation processes, and the proper assessment of subsidence risks. It can also provide critical data for making informed decisions within industries such as oil and gas production.

In this study, the combined or standard models were used to predict UCS. The BP model is a type of neural network where the training process consists of feeding inputs through the network, comparing the output to the desired output, and adjusting the weights of the network iteratively until the desired output is reached. The PSO–BP model uses an optimization algorithm to fine-tune the weights and biases of the neural network. This allows for more efficient training and better performance than a standard BP model. The PSO–LSSVM model is a type of machine learning algorithm that combines the PSO algorithm with the LSSVM regression algorithm. This model can be used for both classification and regression problems, and offers good performance in terms of accuracy and speed.

Overall, the main difference between the three models is that the PSO–BP and PSO–LSSVM models use an optimization algorithm to fine-tune the parameters of the model, which can result in better performance than a

standard BP model. Additionally, the PSO–LSSVM model can be used for both classification and regression problems, while the BP and PSO–BP models are primarily used for classification.

The prediction accuracy of these models can vary depending on the data set and the specific parameters chosen during training. In general, the PSO–BP and PSO–LSSVM models have been shown to offer improved performance over the standard BP model. Studies and experiments have reported that the PSO–BP model has a higher prediction accuracy than the standard BP model in various fields, such as image recognition, fault diagnosis, and stock price forecasting (Mohamad et al., 2018). The PSO–BP model has also been shown to be more robust and less prone to overfitting. Moreover, the PSO–LSSVM model has demonstrated excellent prediction accuracy in a wide range of applications, including classification, regression, and time-series forecasting. The PSO–LSSVM model is particularly effective for high-dimensional data sets, as it can handle large amounts of noise and data complexity.

While the PSO–LSSVM model offers many advantages, such as high prediction accuracy and the ability to handle high-dimensional data sets, there are also some limitations and potential disadvantages to consider.

1) Sensitivity to parameter settings: the PSO–LSSVM model has several parameters that need to be set, such as the regularization parameter and kernel function. If these parameters are not chosen appropriately, the model's performance can suffer. Tuning these parameters can be time-consuming, and it may not always be straightforward to determine the optimal settings.

2) Limited interpretability: like many machine learning models, the PSO–LSSVM model can be difficult to interpret. It can be challenging to understand how specific inputs are influencing the model's output or how the model is making decisions.

3) Computational complexity: the PSO–LSSVM model can be computationally expensive, particularly when dealing with large data sets or complex models. Training the model can take a long time, especially when using a sophisticated optimization algorithm such as PSO.

4) Limited data efficiency: compared to other machine learning models, the PSO–LSSVM model can require large amounts of data to achieve optimal performance. This means that the model may not be well-suited for tasks where data are limited or expensive to obtain.

5) Limited functionality: while the PSO–LSSVM model is a versatile machine learning algorithm, it may not be the best choice for every task. Other models may be better suited for certain types of data or applications, depending on the specific requirements of the problem.

In summary, while the prediction accuracy of each model depends on the specific task and data set, the PSO–BP and PSO–LSSVM models have demonstrated a generally improved performance compared to the standard BP model.

6 Conclusions

Several laboratory test data sets, including rock density, $I_{s(50)}$, V_p, R_n, BTS, SHH, and SSH, were collected on 345 samples for shales, sandstones, granites, and volcanic rocks, etc. By performing simple regression analysis, it was demonstrated that each parameter had an intrinsically connected relationship with UCS. Three models, including BP, PSO–BP, and PSO–LSSVM, were constructed to predict the UCS using these laboratory test data sets. Considering four prediction performance indices, including the R^2, RMSE, VAF, and MSE, the most appropriate model was chosen among the three models. The error analysis revealed that in the PSO–LSSVM model, the four performance indices were superior to those in the other two models; hence, the PSO–LSSVM model outperformed the other prediction models in predicting the UCS of rocks. For the PSO–LSSVM model, the ratios of the predicted UCS to the measured UCS for six data sets were 0.954, 0.982, 0.9911, 0.9956, 0.9995, and 0.993, respectively, indicating that the results were more reasonable when the predicted ratio was close to a value of approximately 1. Moreover, the PSO–LSSVM model also worked well for different rock types from different places and granite with different degrees of weathering. Therefore, the PSO–LSSVM model was suitable for determining the UCS for different rock types.

Acknowledgments The work was funded by the Science and technology program of Xizang Autonomous Region (Nos. XZ202301YD0034C and XZ202202YD0007C); the National Natural Science Foundation of China (Grant No. 42002268); Open Fund of Badong National Observation and Research Station of Geohazards (No. BNORSG-202204).

Conflicts of Interest The authors declare no conflict of interest.

Data availability The data sets generated during and/or analyzed during the current study are available from the corresponding author on reasonable request.

References

Abdi Y, Momeni E, Khabir R R (2020). A reliable PSO-based ANN approach for predicting unconfined compressive strength of sandstones. Open Constr Build Technol J, 14(1): 237–249

Aladejare A E (2020). Evaluation of empirical estimation of uniaxial compressive strength of rock using measurements from index and physical tests. J Rock Mech Geotech Eng, 12(2): 256–268

Jahed Armaghani D, Mohd Amin M F, Yagiz S, Faradonbeh R S, Abdullah R A (2016). Prediction of the uniaxial compressive strength of sandstone using various modeling techniques. Int J Rock Mech Min Sci, 85: 174–186

Asteris P G, Mamou A, Hajihassani M, Hasanipanah M, Koopialipoor M, Le T T, Kardani N, Armaghani D J (2021). Soft computing based closed form equations correlating L and N-type Schmidt

hammer rebound numbers of rocks. Transp Geotechnics, 29: 100588

Cai Z L, Xu W Y, Meng Y D, Shi C, Wang R B (2016). Prediction of landslide displacement based on GA-LSSVM with multiple factors. Bull Eng Geol Environ, 75(2): 637–646

Gowida A, Elkatatny S, Gamal H (2021). Unconfined compressive strength (UCS) prediction in real-time while drilling using artificial intelligence tools. Neural Comput Appl, 33(13): 8043–8054

Hu Z, Wen T, Zheng K, Wang Y (2021). A Method for determining the mechanical parameters of solution pore and crevice limestone based on porosity. Adv Civ Eng, 2021: 1–14

Iyare U C, Blake O O, Ramsook R (2021). Estimating the uniaxial compressive strength of argillites using Brazilian tensile strength, ultrasonic wave velocities, and elastic properties. Rock Mech Rock Eng, 54(4): 2067–2078

Jahed Armaghani D, Tonnizam Mohamad E, Hajihassani M, Yagiz S, Motaghedi H (2016). Application of several non-linear prediction tools for estimating uniaxial compressive strength of granitic rocks and comparison of their performances. Eng Comput, 32(2): 189–206

Li C D, Tang H M, Ge Y F, Hu X L, Wang L Q (2014). Application of back-propagation neural network on bank destruction forecasting for accumulative landslides in the three Gorges Reservoir Region, China. Stochastic Environ Res Risk Assess, 28(6): 1465–1477

Li R, Xu S, Zhou Y, Li S, Yao J, Zhou K, Liu X (2020). Toward group applications of Zinc-Silver battery: a classification strategy based on PSO-LSSVM. IEEE Access, 8: 4745–4753

Li W, Tan Z Y (2016). Comparison on rock strength prediction models based on MLR and LS-SVM. Mining Res Develop, 36(11): 36–40

Liu Z, Jahed Armaghani D, Fakharian P, Li D Y, Vladimirovich Ulrikh D, Nikolaevna Orekhova N, Mohamed Khedher K (2022). Rock strength estimation using several tree-based ML techniques. Comput Model Eng Sci, 133(3): 799–824

Looney C G (1996). Advances in feedforward neural networks: Demystifying knowledge acquiring black boxes. IEEE Trans Knowl Data Eng, 8(2): 211–226

Mohamad E T, Armaghani D J, Momeni E, Yazdavar A H, Ebrahimi M (2018). Rock strength estimation: a PSO-based BP approach. Neural Comput Appl, 30(5): 1635–1646

Mohamad E T, Jahed Armaghani D, Momeni E, Alavi Nezhad Khalil Abad S V (2015). Prediction of the unconfined compressive strength of soft rocks: a PSO-based ANN approach. Bull Eng Geol Environ, 74(3): 745–757

Momeni E, Nazir R, Armaghani D J, Amin M F M, Mohamad E T (2015a). Prediction of unconfined compressive strength of rocks: a review paper. J Teknol, 77(11): 43–50

Momeni E, Jahed Armaghani D, Hajihassani M, Mohd Amin M F (2015b). Prediction of uniaxial compressive strength of rock samples using hybrid particle swarm optimization-based artificial neural networks. Measurement, 60: 50–63

Rahman T, Sarkar K (2021). Lithological control on the estimation of uniaxial compressive strength by the P-Wave velocity using supervised and unsupervised learning. Rock Mech Rock Eng, 54(6): 3175–3191

Skentou A D, Bardhan A, Mamou A, Lemonis M E, Kumar G, Samui P, Armaghani D J, Asteris P G (2023). Closed-form equation for estimating unconfined compressive strength of granite from three non-destructive tests using soft computing models. Rock Mech Rock Eng, 56(1): 487–514

Teymen A, Mengüç E C (2020). Comparative evaluation of different statistical tools for the prediction of uniaxial compressive strength of rocks. Int J Min Sci Technol, 30(6): 785–797

Wang Y, Tang H, Huang J S, Wen T, Ma J, Zhang J (2022). A comparative study of different machine learning methods for reservoir landslide displacement prediction. Eng Geol, 298: 106544

Wen T, Tang H M, Wang Y K, Lin C Y, Xiong C R (2017). Landslide displacement prediction using the GA-LSSVM model and time series analysis: a case study of Three Gorges Reservoir, China. Nat Hazards Earth Syst Sci, 17(12): 2181–2198

Wen T, Hu Z, Wang Y, Zhang Z (2021). Variation law of air temperature of a high-geotemperature tunnel during the construction. Lithosphere, 2021(Special 7) : 2541884

Wen T, Hu Z, Wang Y, Tang R (2023). Genetic mechanism of high geotemperature in tunnels in consideration of temperature monitoring and hydrogeochemical analysis. Environ Sci Pollution Res, 1–17

Wen T, Wang Y K, Tang H M, Zhang J R, Hu M Y (2023). Damage evolution and failure mechanism of red-bed rock under drying–wetting cycles. Water, 15(15): 2684

Xue X H, Xiao M (2017). Deformation evaluation on surrounding rocks of underground caverns based on PSO-LSSVM. Tunn Undergr Space Technol, 69: 171–181

Zhang H J, Wu S C, Zhang Z X (2022). Prediction of uniaxial compressive strength of rock via genetic algorithm—selective ensemble learning. Nat Resour Res, 31(3): 1721–1737

Zhang J R, Lin C Y, Tang H M, Wen T, Tannant D D, Zhang B C (2024). Input-parameter optimization using a SVR based ensemble model to predict landslide displacements in a reservoir area–a comparative study. App Soft Comput, 150: 111107

Zhao L X, Shui P B, Jiang F, Qiu H Q, Ren S M, Li Y K, Zhang Y (2014). Using monitoring data of surface soil to predict whole crop-root zone soil water content with PSO-LSSVM, GRNN and WNN. Earth Sci Inform, 7(1): 59–68

Zhu X, Ma S Q, Xu Q, Liu W D (2018). A WD-GA-LSSVM model for rainfall-triggered landslide displacement prediction. J Mt Sci, 15(1): 156–166